JOURNAL OF SOLID STATE CHEMISTRY 113, 239–247 (1994)

Formation of $BaTiO_3$ from Citrate Precursor

M. Rajendran[1] and M. Subba Rao

Department of Inorganic and Physical Chemistry, Indian Institute of Science, Bangalore, Karnataka 560012, India

Received April 12, 1993; in revised form January 10, 1994; accepted January 12, 1994

On thermal decomposition barium bis(citrato)oxotitanate (IV) citrate heptahydrate produces stoichiometric $BaTiO_3$ fine powders at about 650°C. Thermal decomposition of the precursor proceeds through three major stages, viz. (i) dehydration, (ii) decomposition of the citrate to form an oxycarbonate intermediate $Ba_2Ti_2O_5CO_3$, and (iii) decomposition of the intermediate carbonate to form $BaTiO_3$. Spectroscopic and thermoanalytical techniques are presently employed to characterize the precursor and the intermediates isolated at various stages. As-prepared $BaTiO_3$ is a mixture of cubic and tetragonal phases. The primary particle size of the powder is on the order of 100 nm, as revealed by the TEM technique. Calcining the powders above 800°C results in the formation of complete tetragonal phase with improved crystallinity. The resultant powders are sinter active to give dense monophasic ceramic compacts having densities in the range 95–99% of the theoretical value. Depending on the processing conditions, the dielectric constant (ε_r) varies from 1600 to 3000 at 1 kHz, while the dielectric loss, tan δ, ranges from 0.003 to 0.009 at 300 K.

1. INTRODUCTION

Low-temperature synthesis of $BaTiO_3$ fine powders has attracted considerable interest in recent years due to the technological importance of these powders in the fabrication of ceramic capacitors (1). The small size of the oxide particles enables better sintering and the development of uniform microstructure throughout the ceramic component. The fine-grain feature in the resultant ceramic improves to a large extent the performance and reliability of physical properties. The diffusional limitations and the phase boundary control in solid–solid reactions could be overcome to a remarkable extent by employing a suitable molecular precursor technique to synthesize fine-particle $BaTiO_3$. The molecular precursor approach offers the advantage of achieving an intimate molecular-level mixing of the metal ions in the precursor. On thermal conversion at relatively low temperatures the resultant precursor produces $BaTiO_3$ fine powders possessing desirable powder characteristics, such as phase purity, chemical homogeneity, uniform size, and high surface area.

Citrate complexation is one of the most efficient precursor methods for producing $BaTiO_3$ fine powders. This method requires a relatively low temperature and short duration to produce the oxide (2–5). Also, this technique effectively removes the common impurities, e.g., Sr, Ca, and Nb, besides keeping the Ba : Ti ratio at exactly one in the precursor (5). This process was developed by Pechini, and the pathway to the oxide formation was found to proceed through a route other than through $BaCO_3$ and TiO_2 intermediates (2). The preparative condition was modified by Mulder to obtain the precursor, $BaTi(C_6H_6O_7)_3 \cdot 4H_2O$, via an alcohol dehydration process (3). The effect of pH on Ba : Ti content of the precursor and the thermal decomposition characteristics of BaTi $(C_6H_6O_7)_3 \cdot 6H_2O$ have been reported by Hennings and Mayr (4). Prior to the formation of $BaTiO_3$, $BaCO_3$ and TiO_2 have been identified as intermediates in the latter work.

All these investigations ascertain the formation of monophasic $BaTiO_3$ fine powders from citrate precursors but contradict each other in formulating the precursor composition and the pathway to the oxide formation. In addition, a metastable hexagonal phase has been identified in citrate-derived $BaTiO_3$ powders (6), though the low-temperature syntheses usually stabilize the cubic phase. However, studies on the phase evolution feature and the thermal stability of the metastable phases are still lacking. Also, the dielectric properties of ceramic compacts processed by the citrate method have not been adequately characterized.

Therefore, the main objective of the present study is to provide the results of a systematic investigation on the genesis of $BaTiO_3$ from the citrate precursor barium bis(citrato)oxotitanate (IV) citrate heptahydrate (BTCC). The variation of the dielectric constant (ε_r) as a function of processing temperature has been investigated for the ceramic compacts. For comparison, the results obtained for the compacts processed through the ceramic method and the alkoxide route are also presented.

[1] To whom correspondence should be addressed. Present address: Materials Science Research Center, Indian Institute of Technology, Madras 600036, India.

0022-4596/94 $6.00

2. EXPERIMENTAL DETAILS

Materials

Preparation of $BaTiO(C_6H_6O_7)_2$ $(C_6H_8O_7)\cdot 7H_2O$ (BTCC). Tetraisopropyl orthotitanate (25 ml) is added to an aqueous solution of citric acid (46.457 g in 50 ml H_2O) and warmed to get a clear solution. To this is added an aqueous solution of barium chloride (18 g of $BaCl_2\cdot 2H_2O$ in 50 ml H_2O) so that the mole ratio of Ba : Ti : citrate = 1 : 1 : 3. On leaving the above mixture at room temperature for 2 days, BTCC precipitates out. The precipitate is filtered, washed with deionized water, and vacuum dried.

Citrate content in BTCC is estimated by decomposing the complex in $2N$ H_2SO_4, and the liberated citric acid is estimated by oxidation with a known excess of ceric sulfate solution. Barium sulfate precipitated out in the above process is filtered and estimated gravimetrically for barium content. Titanium content is estimated by precipitating titanium with cupferron, followed by incineration to TiO_2. From these estimations the water content is computed for a known quantity of the sample.

Preparation of $BaTiO_3$ by the alkoxide route. Tetraisopropyl orthotitanate (25 ml) is diluted in 200 ml of isopropanol. The titanium content is estimated by hydrolysis of a known quantity of the alkoxide solution followed by incineration of the hydrous titania to TiO_2. Dropwise addition of the alkoxide solution to an aqueous solution of warm barium hydroxide (23.247 g $Ba(OH)_2\cdot 8H_2O$ in 450 ml water) is carried out in CO_2 free atmosphere with constant stirring. The resultant mixture is digested at 100°C for 5 hr under a nitrogen blanket. The solvent is evaporated and the powder is calcined at 650°C to produce $BaTiO_3$.

Preparation of $BaTiO_3$ by the ceramic method. Stoichiometric quantities of high-purity $BaCO_3$ and TiO_2 powders are mixed thoroughly under acetone and heated at about 1050°C for 24 hr with intermittent grindings.

Physical Methods

Thermoanalytical studies were carried out using a commercial Ulvac TA-1500 simultaneous TG-DTA-DTG thermal analyzer with a heating rate of 20°C/min on 5–8 mg of samples. Powder X-ray diffraction was recorded on a Philips PW 1050/70 diffractometer employing nickel-filtered copper radiation and a scan rate of 2° per minute. Transmission electron microscope (Philips EM-301 model) was used for electron diffraction (ED) studies. Surface area was measured with a Micromeritics Accusorb (2100E) instrument. IR spectra in the range 200–4000 cm^{-1} were recorded with a Perkin–Elmer (PE) Model 597, double-beam spectrometer. The samples were prepared in spectral-grade KBr pellets. Solid-state ^{13}C NMR spectra were recorded on a Bruker MSL-300 spectrometer operating at 75.47 MHz. The chemical shifts are referenced to external TMS. The spectra were recorded at the spinning rates of 3 and 3.5 kHz for each sample to identify the spinning sidebands. Temperature programmed decomposition spectra (TPDS) of the samples were performed in a modified GC-MSD system HP5890-5970. In a TPDS experiment, the sample was heated at a constant rate of 20°C/min in a stream of helium. The volatile gaseous decomposition products were analyzed on-line using a quadrupole mass spectrometer. Scanning electron micro-

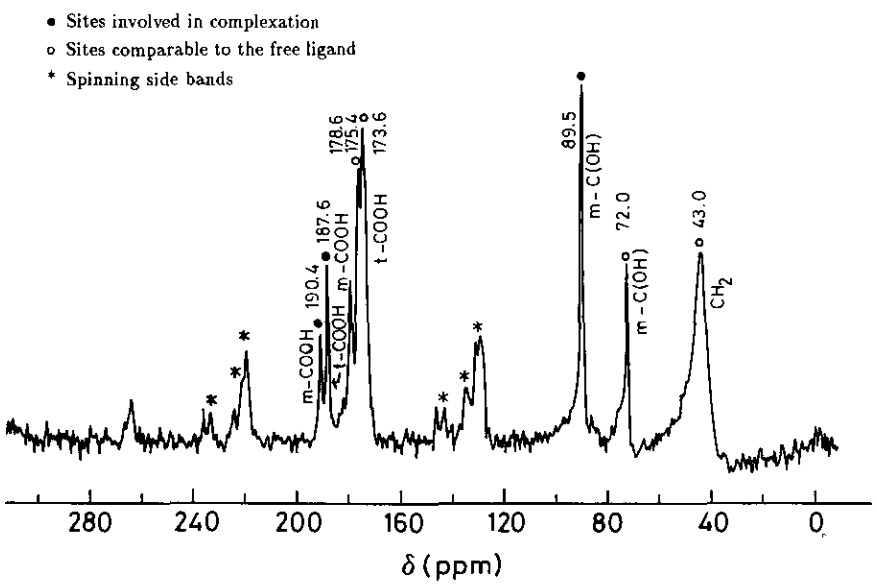

FIG. 1. Solid-State ^{13}C NMR spectrum of BTCC.

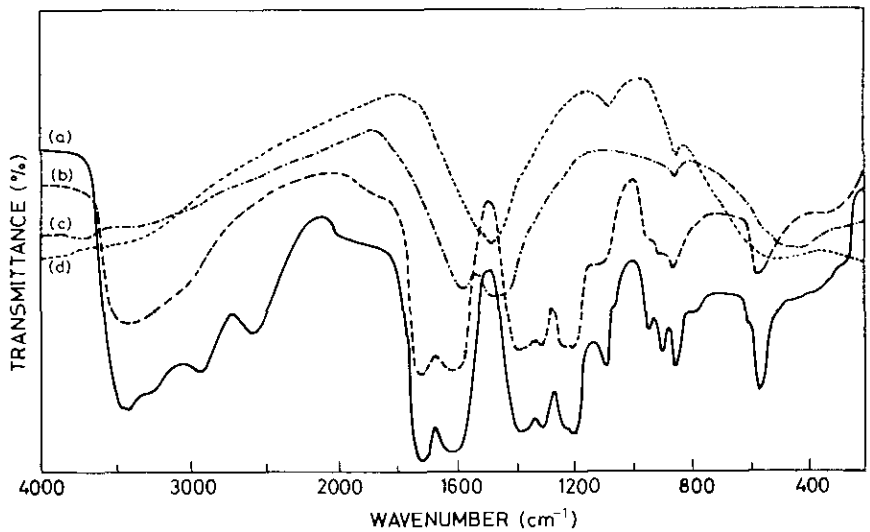

FIG. 2. IR spectra of (a) BTCC and the intermediates isolated at (b) 150, (c) 400, and (d) 550°C.

graphs were obtained from Cambridge Stereoscan (Model S-150). A Genrad GR 1658 automatic digital bridge was used for the capacitance measurements. Accuracy of the instrument was ±0.1%. The amplitude of the applied sinusoidal signal was 0.4 V cm^{-1}. The dielectric sample was coated with nickel by electroless nickel plating for electrical contact. The temperature of the specimen was varied from 25 to 200°C at a rate of 1°C/min. From the measured value of capacitance (C), ε_r was calculated from the relation

$$C = \frac{\varepsilon_0 \varepsilon_r A}{d},$$

where ε_r is the relative permittivity, ε_0 is the permittivity of vacuum, A is the area of the sample, and d is the thickness of the sample.

3. RESULTS AND DISCUSSION

Characterization of the Precursor BTCC

Chemical analysis of BTCC gives the following: Ba^{2+} = 15.26, TiO^{2+} = 7.10, citrate = 62.59, and H_2O = 14.26%, in agreement with the calculated values of Ba^{2+} = 15.28, TiO^{2+} = 7.11, citrate = 63.58, and H_2O = 14.03%.

The solid-state ^{13}C NMR spectrum of BTCC is shown in Fig. 1. ^{13}C resonance absorptions of the carboxyl groups show the presence of both coordinated and free carboxyl groups. The central carbon, C(OH), also gives rise to two resonance absorptions, one corresponding to the free ligand and the other to a down-field shift, indicating its involvement in complexation. The signals corresponding to the functional groups of the free ligand reveal the presence of ligand sites not involved in complexation. The respective chemical-shift values corresponding to the resonance absorptions of various ^{13}C sites are also given in the figure.

The IR spectrum of BTCC shows the presence of both coordinated and free carboxylate groups (Fig. 2). The coordinated carboxylate group gives rise to ν_{as} (COO) at 1610 cm^{-1} and ν_s (COO) at 1370 cm^{-1}, whereas the free carboxylate group shows the typical absorptions, ν_{as} (COO) and ν_s (COO) at 1730 and 1400 cm^{-1}, respectively. The difference between the asymmetric and the symmetric COO stretching modes. $\Delta(\nu_{as} - \nu_s)$, of the coordinated carboxylate groups, is on the order of 240 cm^{-1}. This magnitude suggests the unidentate coordination of the carboxylate groups (7, 8).

In aqueous medium as well as in solid state, the titanyl and zirconyl species exist as polymeric (–*M*–O–*M*–) (*M* = Ti or Zr) bridging groups. Since BTCC is crystallized in aqueous solution it is more likely that the complex contains a polymeric (–Ti–O–Ti–) chain analogous to the titanyl oxalate (9). Excessive ligand concentration can favor the precipitation of metal carboxylates containing carboxylic acid of crystallization as in the case of $Ba(C_2O_4) \cdot (H_2C_2O_4) \cdot 2H_2O$ (10). Similarly it is inferred from the spectral and the thermoanalytical studies that BTCC is likely to have the free ligand of crystallization. From these results and chemical analysis the composition of BTCC is formulated as $BaTiO(C_6H_6O_7)_2 \cdot C_6H_8O_7 \cdot 7H_2O$. In BTCC, two citrates chelate to one titanium, with each citrate coordinating through two unidentate carboxylate groups, while the rest of the coordination sphere is completed by two bridging oxygen atoms to give titanium a sixfold coordination.

Thermal Decomposition of Citric Acid

Since the precursor may follow the thermal decomposition pathways of the ligand, the decomposition of citric acid has also been investigated. Figures 3a and 3b are the DTA traces of citric acid monohydrate recorded at a

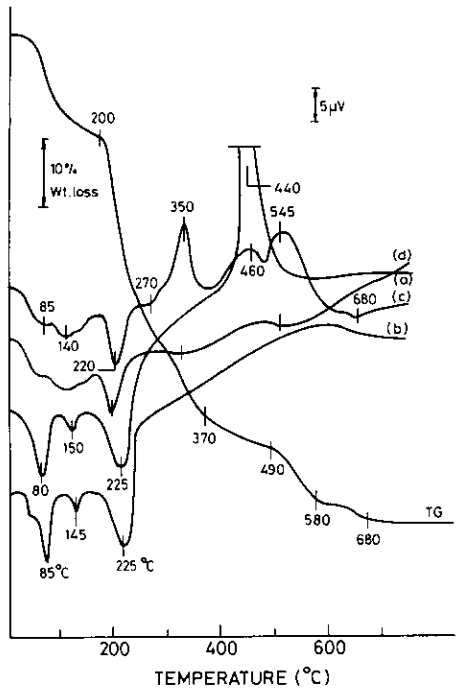

FIG. 3. TG of BTCC and DTA of (a) citric acid in air, (b) citric acid in argon, (c) BTCC in air, and (d) BTCC in argon.

heating rate of 20°C/min in static air and flowing argon atmosphere, respectively. The endotherms at 80, 150, and 225°C (Fig. 3) represent the following thermal events: dehydration, melting, and the initial stage of decarboxylation to evolve CO_2 as the primary decomposition product. These events are not significantly affected by the surrounding atmosphere.

The rate of heating decides the further course of decomposition, and the sequence of thermal events is illustrated in Fig. 4. The DTA results are supported by the TPDS. The primary thermolysis products (Fig. 5) are identified from their typical *m/e* values.

The present study suggests the following sequence for citric acid decomposition when a heating rate of less than 50°C/min is employed: citric acid → aconitic acid → itaconic acid → itaconic anhydride.

The further course of decomposition is represented by an intense exotherm at 440°C in static air (Fig. 3a). Reduced oxygen partial pressures, P_{O_2}, causes a shift in the position of the exotherm to higher temperatures. The above thermal event disappears in nonoxidizing atmospheres to give a charred mass. These results demonstrate the importance of an oxidizing atmosphere for complete decomposition of citric acid.

Thermal Decomposition of BTCC

Thermal decomposition of BTCC occurs in three major stages, (i) dehydration, (ii) decomposition of the citrate to form an ionic carbonate intermediate, and (iii) the de-

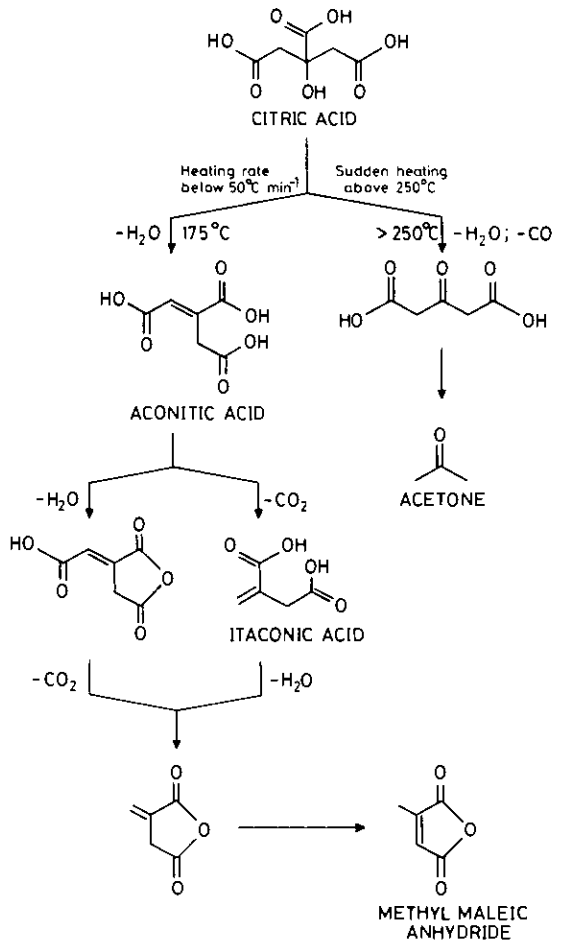

FIG. 4. Thermal decomposition sequence of citric acid.

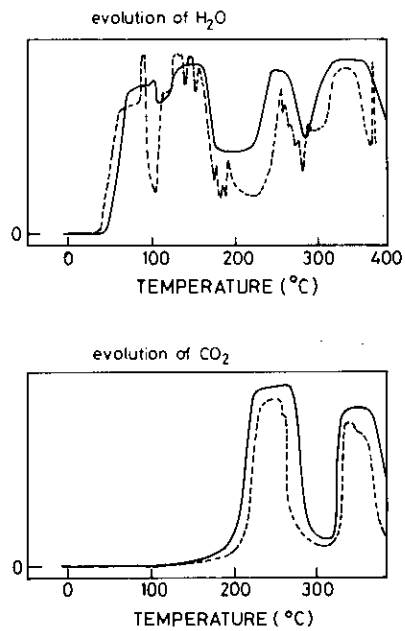

FIG. 5. TPDS spectra of citric acid (---) and BTCC (—).

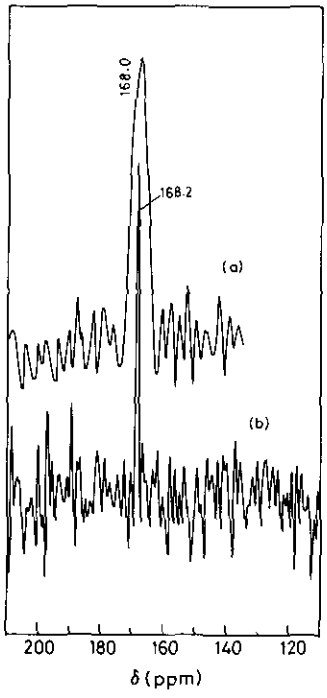

FIG. 6. ^{13}C NMR spectra of (a) $Ba_2Ti_2O_5CO_3$ and (b) $BaCO_3$.

composition of the mixed metal carbonate to form barium titanate.

(*i*) *Dehydration process.* A TG weight loss of 14% is recorded for the dehydration process, which corresponds to the removal of $7H_2O$/mole of the precursor, in agreement with the calculated value of 14.03%. The dehydration process consists of two steps, as can be inferred from the position of the endotherms in DTA centred around 85 and 140°C (Fig. 3). The residue isolated by isothermal calcination of BTCC at 140°C for 5 hr showed a change in weight corresponding to the removal of $7H_2O$ per mole of the precursor. This temperature is 60°C lower than the value reported in an earlier investigation (4) for the dehydration process. Contrary to the previous report, no thermal effect is shown in DTA in the temperature range 150–200°C, except a weak endotherm at 150°C. The thermal effect at 150°C is likely to be due to the melting of citric acid, originating from the partial decomplexation of the precursor during dehydration.

(*ii*) *Thermal decomposition of citrate.* Further decomposition of BTCC is found to be a simultaneous decomposition of the citrate and the citric acid liberated from the complex, as shown in Fig. 3. The endotherm at 220°C is attributed to the thermal decarboxylation of citric acid to evolve CO_2 as the primary decomposition product. An aqueous extract of the residue isolated at this stage gives a positive test for unsaturation, revealing the presence of itaconic acid. A weak endotherm at 270°C corresponds to the decomposition of the complexed citrate. The decomposition proceeds further to give exotherms at 350, 460, and 545°C. The exotherms representing the thermal events at 350 and 545°C are due to the decomposition of intermediate carboxylates, and the one at 460°C is attributed to the combustion of the thermolysis products of itaconic acid.

In nonoxidizing atmospheres, the above thermal events appear as broad, weak endotherms centered around 355 and 550°C, with considerable carbonization.

BTCC gives a TG weight loss of 72% in the temperature

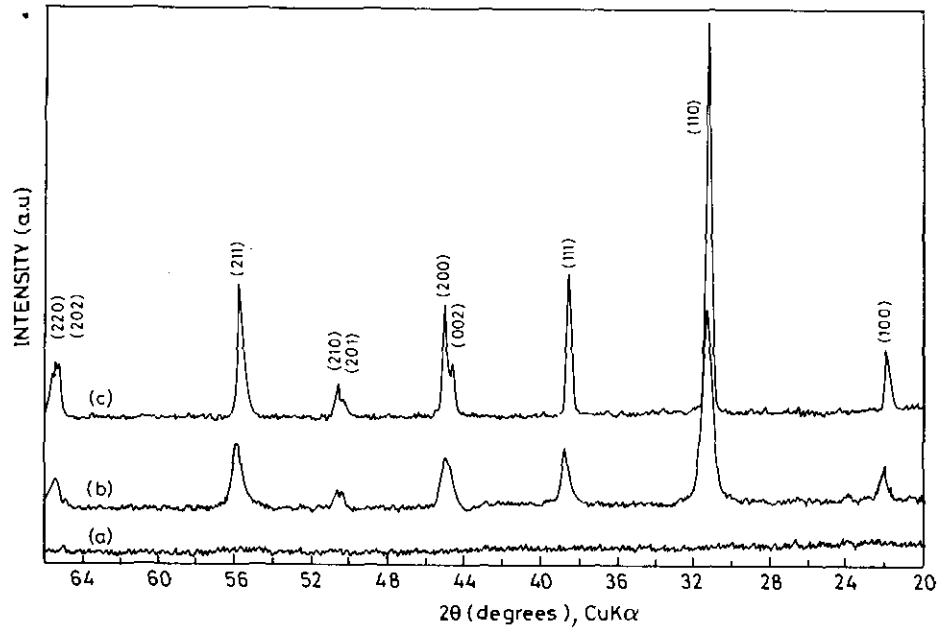

FIG. 7. XRD patterns showing the progressive stages of $BaTiO_3$ formation from BTCC at (a) 500, (b) 650, and (c) 800°C.

range 580–680°C to give a stable intermediate. The chemical analysis of the above residue suggests that the composition of this intermediate is $Ba_2Ti_2O_5CO_3$. A similar intermediate has also been isolated during the thermal decomposition of barium titanyl oxalate (11). The present study does not substantiate the demixing of barium and titanium.

(iii) Thermal decomposition of the intermediate carbonate to barium titanate. A weak endotherm at 680°C in DTA (Fig. 3) represents the decomposition of the intermediate carbonate with the evolution of carbon dioxide to give barium titanate. The TG recorded in air shows a weight loss of 74.0%, in agreement with the calculated value of 74.05% for BTCC to form the oxide. Isothermal calcination of $Ba_2Ti_2O_5CO_3$ in the temperature range 650–700°C for about 5 hr gives a weight loss of 8.6% to produce $BaTiO_3$. The final weight-loss step and the corresponding thermal effect support the decomposition of $Ba_2Ti_2O_5CO_3$ rather than the solid-state reaction between $BaCO_3$ and TiO_2 to produce $BaTiO_3$.

Characterization of the Intermediates of Thermal Decomposition

IR spectral results. IR spectra of the intermediates isolated at different temperatures are given in Fig. 2. The residue isolated at 150°C for 2 hr shows reduction in $\nu_{(O-H)}$ due to the elimination of water, while the intensities of the carboxylate bands remain the same as that of the precursor. Calcination of BTCC at 225°C for 3 hr results in a considerable decrease in the intensity of free carboxylate absorption at 1730 cm^{-1}. An aqueous extract of this residue gives a positive test for unsaturation. However, the free carboxylate stretching mode is completely absent for the residue isolated at 350°C. An increase in the decomposition temperature to 400°C yields a residue which shows both coordinated carboxylate and ionic carbonate bands at ~1590 and ~1450 cm^{-1}, respectively. At 550°C only the ionic carbonate bands are seen in the IR spectrum. Chemical analysis of the resultant intermediate suggests the composition $Ba_2Ti_2O_5CO_3$. Unlike oxalate precursors, none of the intermediates obtained from the citrate precursor, BTCC, give evidence for the presence of entrapped CO_2 (11).

TABLE 1
Powder Characteristics of $BaTiO_3$ Obtained from Different Methods

Powder characteristics	BTCC	Alkoxide	Ceramic
Formation temperature (°C) and duration	650, 7 hr	650, 7 hr	1050, 24 hr
Phase content	Cubic and tetragonal	Cubic	Tetragonal
Primary particle size[a] (μm)	0.1	0.05	2.0 to 5.0
Average agglomerate size (μm)	2.0	1.0	—
Surface area[b] ($m^2\ g^{-1}$)	15.0	21.0	1.5
Presence of second phase[c]	—	—	Ba_2TiO_4 (trace)

[a] From TEM.
[b] BET method.
[c] Powder XRD.

TABLE 2
Physical Properties of $BaTiO_3$ Ceramics Processed from Powders Obtained by Different Methods

Method of powder preparation and processing conditions	Density of the ceramic (%)	Average grain size (μm)	Dielectric constant at 300 K and 1 kHz	Tan δ at 300 K and 1 kHz
		Ceramic route		
As compacted	55	—	—	—
1300°C, 2 hr	81	3.0	1400	0.015
1350°C, 2 hr	87	45.0	1300	0.009
		Citrate complex		
As compacted	64	—	—	—
1275°C, 2 hr	86	0.5	2000	0.009
1300°C, 2 hr	92	0.8	3000	0.005
1300°C, 5 hr	99	1.0	1800	0.003
1330°C, 2 hr	99	2.0	1600	0.009
		Alkoxide route		
As compacted	65	—	—	—
1275°C, 2 hr	90	0.5	1600	0.004
1300°C, 2 hr	95	2.0	1200	0.005
1300°C, 5 hr	99	2.0	1300	0.003
1330°C, 2 hr	98	12.0	1400	0.005

Results of TPDS. The sequence of thermal events has been probed using the TPDS technique for the free ligand and the complex at a heating rate of 20°C/min. The released primary thermolysis products at the early stages have been identified from their characteristic *m/e* values. The free ligand evolves water at about 85°C and 140–170°C. In addition, CO_2 evolution is noted at 220°C. For the precursor, water evolution takes place at 85, 140, 170, and 270°C, while CO_2 is evolved at 220°C (Fig. 5). The presence of the free ligand in the precursor BTCC at the early stages of decomposition can be inferred from the overlapping and relatively wider thermal events, which compliment the results of DTA.

^{13}C NMR investigation. The solid-state ^{13}C NMR spectrum of the intermediate isolated at 500°C for 10 hr is shown in Fig. 6. A broad resonance absorption at about 168 ppm, characteristic of an ionic carbonate, is observed. For comparison, the ^{13}C NMR spectrum of the residue isolated by calcining the mechanical mixture of barium citrate and titanyl citrate at 500°C for 10 hr is also shown in Fig. 6. The sharp resonance absorption in this case is

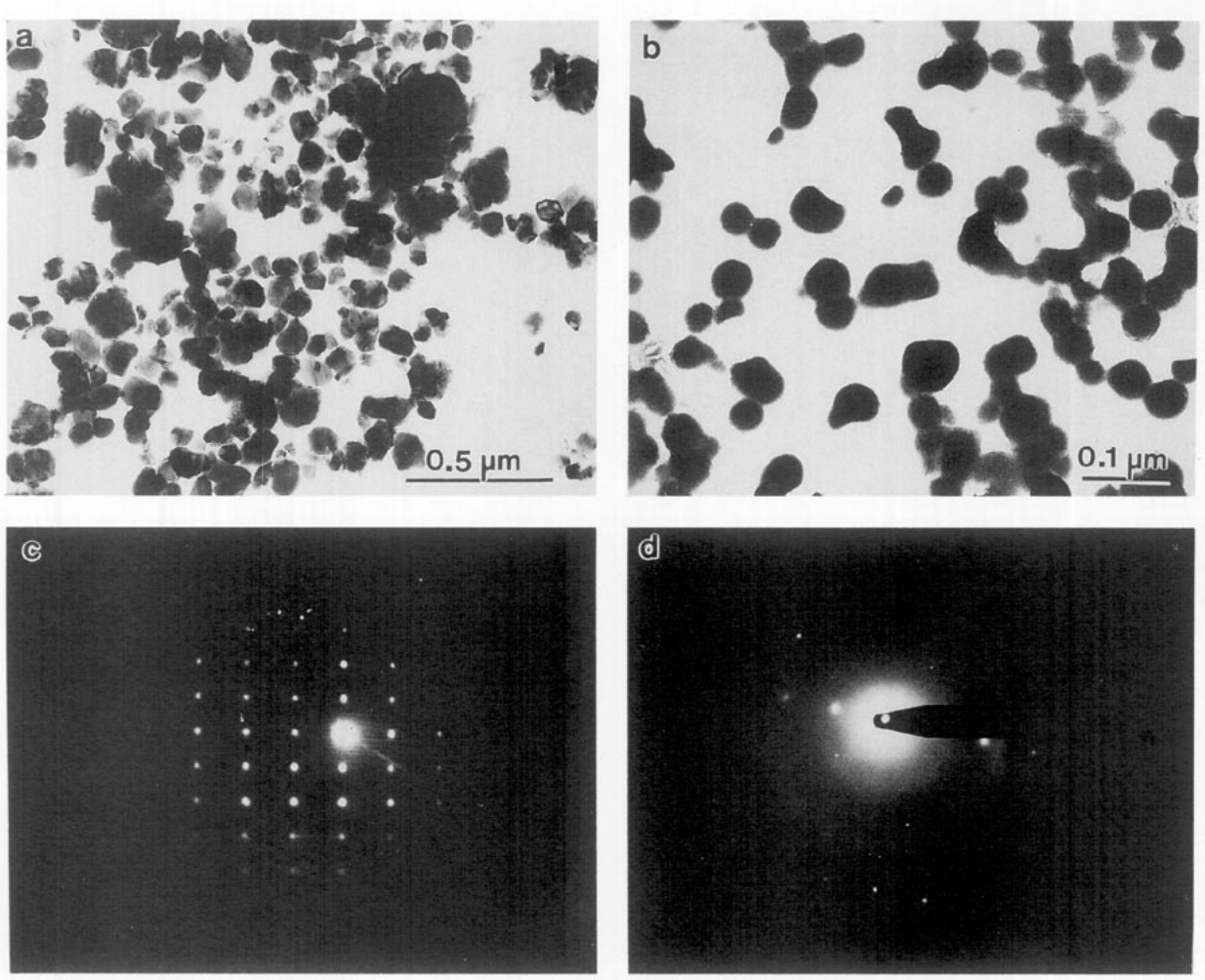

FIG. 8. Transmission electron micrographs of $BaTiO_3$ powders obtained from (a) BTCC and (b) alkoxide routes after heat treatment at 800°C for 1 hr. (c, d) The corresponding ED patterns.

due to $BaCO_3$. Though the peak positions are comparable (Figs. 6a and 6b), considerable difference is shown in their linewidth. Since the chemical analysis and other techniques have suggested the absence of $BaCO_3$, the ^{13}C resonance feature in the present case is attributed to the ionic carbonate intermediate, $Ba_2Ti_2O_5CO_3$.

Powder XRD studies. An X-ray diffraction study on the intermediates obtained by the thermal decomposition of BTCC reveals their amorphous nature, including the one isolated at 550°C. This observation contradicts the results of Hennings and Mayr (4). These authors have reported the presence of $BaCO_3$ and a poorly crystalline intermediate along with $BaTiO_3$ for the residue isolated at 500°C. Neither $BaCO_3$ nor any other crystalline intermediate is identified from the XRD pattern of the residue in the present study. Calcination of the precursor in the range 600–650°C results in the formation of $BaTiO_3$ as the only product (Fig. 7). The mixed-phase (cubic and tetragonal) nature of this powder is inferred from the X-ray diffraction pattern. The broad asymmetric peak profile at $2\theta = 45°$ (Cu$K\alpha$) corresponds to both cubic, (200), and tetragonal, (200) and (002), reflections. At higher angles, the corresponding reflections (400) for cubic and (400) and (004) for tetragonal phases are found to be well separated, as in the case of the oxalate-derived sample (13).

Thermal treatment of the sample above 800°C gives good crystallinity and complete conversion of the powders to the tetragonal phase (Fig. 7c).

Eror *et al.* (6) have observed the hexagonal $BaTiO_3$ phase for the citrate-gel-derived samples. However, the present study does not substantiate this report. Since this discrepancy may be due to the nature of the precursor employed (12), the citrate-gel precursor is also investigated. However, the XRD of the gel-derived $BaTiO_3$ is also similar to that obtained from BTCC.

Thermal Decomposition Scheme for BTCC

From the above results the following scheme can be proposed for the thermal decomposition of BTCC:

$$BaTiO(C_6H_6O_7)_2 \cdot (C_6H_8O_7) \cdot 7H_2O \xrightarrow{25\text{–}140^\circ C}$$

$$BaTiO(C_6H_6O_7)_2 + C_6H_8O_7 + 7H_2O$$

barium titanyl citrate

$$C_6H_8O_7 \xrightarrow{170^\circ C} C_6H_6O_6 + H_2O$$

aconitic acid

$$C_6H_6O_6 \xrightarrow{220^\circ C} C_5H_6O_4 + CO_2$$

itaconic acid

$$C_5H_6O_4 \xrightarrow{>220^\circ C} \begin{matrix} CH_2CO \\ | \quad \diagdown \\ C\text{–}CO \quad O + H_2O \\ \| \quad \diagup \\ CH_2 \end{matrix}$$

itaconic anhydride

$$BaTiO(C_6H_6O_7)_2 \xrightarrow[-CO_2,\,-H_2O]{140\text{–}350^\circ C} BaTiO(C_5H_4O_4)_{2-x}(CO_3)_x \quad (0.2 \le x \le 0.5)$$

$$2BaTiO(C_5H_4O_4)_{2-x}(CO_3)_x \xrightarrow[-H_2O,\,-CO_2,\,-CO]{350\text{–}550^\circ C} Ba_2Ti_2O_5CO_3$$

$$Ba_2Ti_2O_5CO_3 \xrightarrow[-CO_2]{550\text{–}680^\circ C} BaTiO_3.$$

Characterization of Citrate-Derived $BaTiO_3$

The powder characteristics of $BaTiO_3$ obtained from BTCC, alkoxide, and ceramic methods are shown in Table 1. The importance of the nonconventional powder synthesis techniques is shown in Table 2. The particle size of the BTCC-derived powder is comparable to that of the alkoxide method. The TEM of BTCC- and alkoxide-derived $BaTiO_3$ and the corresponding ED patterns are shown in Fig. 8. The good crystallinity of the citrate-derived powder is clearly shown in its monocrystal spot pattern. The alkoxide-derived sample requires a relatively higher calcination temperature to give a monocrystalline diffraction pattern.

Dielectric Properties of $BaTiO_3$ Ceramics Processed from BTCC

$BaTiO_3$ powders are compacted (using 1% polyvinyl alcohol as the binder) and sintered in the temperature range 1250–1350°C. Ohmic contacts are provided using electroless nickel plating. Since the presence of moisture introduced during nickel plating can affect the dielectric properties of $BaTiO_3$ to a considerable extent, the cell assembly is first heated to about 200°C in flowing argon and then cooled to room temperature prior to the measurements.

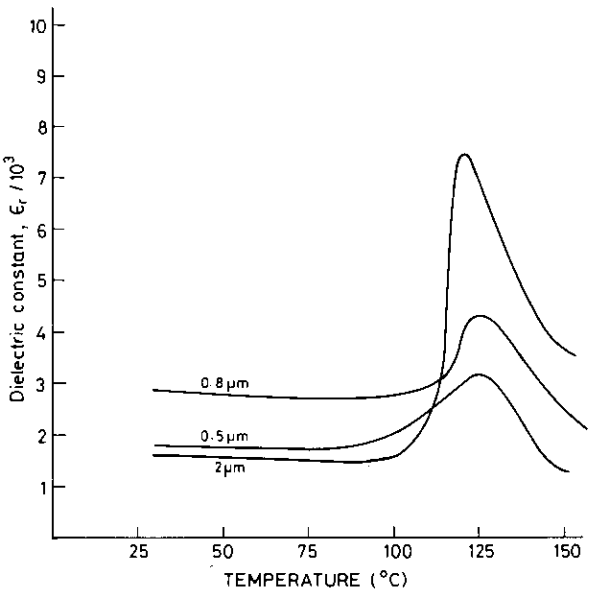

FIG. 9. ϵ_r–T characteristics of BTCC-derived $BaTiO_3$ ceramics having different grain sizes.

The variation of the dielectric constant, ϵ_r, with temperature for the samples having different grain sizes is shown in Fig. 9. The magnitude of the dielectric constant varies from 1600 to 3000. The ceramics having a grain size of 2 μm and above show an almost constant ϵ_r value of about 1600. A decrease in the grain size to 0.8 μm enhances the dielectric constant to the maximum of about 3000. However, a further decrease in the grain size to 0.5 μm or below lowers the dielectric constant. In addition, significant widening of the ferroelectric to paraelectric transition is also noted. These variations in the dielectric properties of fine-grained $BaTiO_3$ have been attributed to the ferroelectric domain size and stress effects (13). For comparative purposes, it is to be noted that the dielectric constant of the single crystalline specimen, $\epsilon_{r,\parallel}$ and $\epsilon_{r,\perp}$ (ϵ_r measured parallel ($\parallel$) and perpendicular ($\perp$) to the c-axis), is on the order of 200 and 4000, respectively (14). For the polycrystalline sample having a mean grain size $\bar{d} \le 1$ μm, a highest ϵ_r value of ~6000 is reported (15). However, BTCC-derived powders on appropriate processing shows a maximum ϵ_r value of about 3000, which is relatively higher than that of the ceramics obtained from the ceramic and alkoxide routes in the present study.

4. CONCLUSIONS

The formation of $BaTiO_3$ from the precursor BTCC has been investigated by employing spectroscopic and

thermoanalytical techniques. The differential thermogram of BTCC contains the thermal events of both the free ligand and the citrate complex. The primary thermolysis products have been identified by employing mass spectrometry. The chemical analysis, thermogravimetric analysis, and powder X-ray diffraction studies do not substantiate the formation of $BaCO_3$ and TiO_2 as intermediates. Instead, formation of an oxycarbonate intermediate, $Ba_2Ti_2O_5CO_3$, is supported from the present investigation. Stoichiometric $BaTiO_3$ powders are obtained at about 650°C. The citrate—derived powders are sinter active to give monophasic, dense ceramic compacts of near-theoretical density.

ACKNOWLEDGMENTS

The authors gratefully acknowledge Drs. S. Vasudevan and M. Jayamurthy for help in TPDS experiments. Thanks are also due to Professor S. S. Krishnamurthy for his valuable suggestions and encouragement.

REFERENCES

1. P. P. Phule and S. H. Rispud, *J. Mater. Sci.* **25,** 1169 (1990).
2. M. Pechini, U.S. Patent No. 3, 330, 697, July, 1967.
3. B. J. Mulder, *Am. Ceram. Soc. Bull.* **49,** 990 (1970).
4. D. Hennings and W. J. Mayr, *J. Solid State Chem.* **26,** 329 (1978).
5. G. A. Hutchins, G. H. Maher, and S. D. Ross, *Am. Ceram. Soc. Bull.* **66,** 681 (1987).
6. N. G. Eror, T. M. Loehr, and B. C. Cornilsen, *Ferroelectrics* **28,** 321 (1980).
7. G. B. Deacon and R. J. Philips, *Coord. Chem. Rev.* **33,** 227 (1980).
8. C. Djordjevic, M. Lee, and E. Sinn, *Inorg. Chem.* **28,** 719 (1989).
9. G. M. H. Van de Velde, S. Harkema, and P. J. Gellings, *Inorg. Chim. Acta* **11,** 243 (1974).
10. J. C. Mutin, G. Watelle, and Y. Dusausoy, *J. Solid State Chem.* **27,** 407 (1979).
11. H. S. Gopalakrishnamurthy, M. Subba Rao, and T. R. Narayanan Kutty, *J. Inorg. Nucl. Chem.* **37,** 891 (1975).
12. M. Rajendran and M. Subba Rao, *Bull. Mater. Sci.* **14,** 367 (1991).
13. G. Arlt, D. Hennings, and G. D. With, *J. Appl. Phys.* **58,** 1619 (1985).
14. W. J. Merz, *Phys. Rev.* **76,** 1221 (1949).
15. R. J. Brandmayr, A. E. Brown, and A. M. Dunlap, *U.S. Technical Report No.* ECOM-2614, May, 1965.